

Coincidence between energy gaps and Kohn anomalies in conventional superconductors

S. Johnston,^{1,2} A. P. Sorini,^{2,*} B. Moritz,^{2,3} T. P. Devereaux,^{2,4} and D. J. Scalapino⁵

¹IFW Dresden, P.O. Box 27 01 16, D-01171 Dresden, Germany

²Stanford Institute for Materials and Energy Science, SLAC National Accelerator Laboratory and Stanford University, Stanford, California 94305, USA

³Department of Physics and Astrophysics, University of North Dakota, Grand Forks, North Dakota 58202, USA

⁴Geballe Laboratory for Advanced Materials, Stanford University, Stanford, California 94305, USA

⁵Department of Physics, University of California, Santa Barbara, California 93106-9530, USA

(Received 22 June 2011; revised manuscript received 2 September 2011; published 23 November 2011)

Recently, neutron scattering spin-echo measurements have provided high-resolution data on the temperature dependence of the linewidth $\Gamma(\mathbf{q}, T)$ of acoustic phonons in conventional superconductors Pb and Nb [see P. Aynajian *et al.*, *Science* **319**, 1509 (2008)]. At low temperatures, the merging of the $2\Delta(T)$ structure in the linewidth with a peak associated with a low-lying $\hbar\omega_{\mathbf{q}_{KA}}$ Kohn anomaly suggested a coincidence between $2\Delta(0)$ and $\hbar\omega_{\mathbf{q}_{KA}}$ in Pb and Nb. Here we carry out a standard BCS calculation of the phonon linewidth to examine its temperature evolution and explore how close $2\Delta(0)/\hbar\omega_{\mathbf{q}_{KA}}$ must be to unity in order to be consistent with the neutron data.

DOI: 10.1103/PhysRevB.84.174523

PACS number(s): 74.20.Fg, 74.25.Kc

I. INTRODUCTION

Using resonant spin-echo neutron scattering techniques, Aynajian *et al.*¹ have recently measured the linewidth of transverse acoustic phonons in high-purity single crystals of Pb and Nb. At low temperatures, which are, however, above the superconducting transition temperature T_c , a plot of the phonon linewidth $\Gamma(\mathbf{q}, T)$ as a function of the phonon wave vector \mathbf{q} exhibits peaks that arise from Kohn anomalies.² When the temperature decreases below T_c and the superconducting gap opens, one sees an expected decrease in the linewidth $\Gamma(\mathbf{q}, T)$ for phonons having energy $\hbar\omega_{\mathbf{q}}$ less than twice the superconducting gap $\Delta(T)$. As $\hbar\omega_{\mathbf{q}}$ approaches $2\Delta(T)$, there is a rapid increase in $\Gamma(\mathbf{q}, T)$ associated with the peak in the quasiparticle density of states at the gap edge and the fact that the BCS coherence factor for a phonon to break a Cooper pair and decay into two quasiparticles approaches 1 at threshold.³ However, as Aynajian *et al.* note, what is surprising is that as T goes to zero, the feature in $\Gamma(\mathbf{q}, T)$ that is associated with $\hbar\omega_{\mathbf{q}} = 2\Delta(T)$ appears to merge with a Kohn anomaly peak. This behavior is seen in both Pb and Nb, posing the following question: Why should the energy of a transverse acoustic phonon associated with a normal state Kohn anomaly coincide with twice the limit of the low-temperature superconducting gap $2\Delta(0)$?

Motivated by this experimental result, we have carried out a standard BCS calculation of the temperature dependence of the transverse acoustic linewidth and examined what happens if $2\Delta(0)$ is near the energy associated with a normal state Kohn anomaly in $\Gamma(\mathbf{q}, T)$. In particular, we are interested in the evolution of $\Gamma(\mathbf{q}, T)$ as the temperature is lowered and $2\Delta(T)$ approaches the energy of the Kohn anomaly $\hbar\omega_{\mathbf{q}_{KA}}$. How close to $\hbar\omega_{\mathbf{q}_{KA}}$ does the low-temperature limit of $2\Delta(T)$ need to be for it to appear that the $2\Delta(0)$ structure in $\Gamma(\mathbf{q}, T)$ merges with the Kohn anomaly structure as T goes to zero?

II. FORMALISM

We begin by first examining the matrix elements for the electron coupling to the transverse acoustic modes.

In clean materials, the coupling of the electrons to the low-frequency transverse phonons occurs through umklapp scattering processes.⁴ As one knows, this is because the polarization $\hat{\epsilon}_\lambda(\mathbf{q})$ of a transverse phonon is orthogonal to \mathbf{q} . In Figs. 1(a) and 1(b), we show Fermi surface sections for Pb and Nb, respectively, obtained from density functional theory (DFT) calculations (ABINIT).⁵ In both cases the calculated Fermi surfaces agree well with measurements.^{6,7} In the top figure for Pb, an umklapp scattering process is shown in which an electron is scattered from \mathbf{k} to $\mathbf{k}' = \mathbf{k} + \mathbf{K}_n + \mathbf{q}$, with \mathbf{q} the wave vector of the transverse phonon and \mathbf{K}_n a reciprocal-lattice vector. In this case, the phonon wave vector \mathbf{q}_{KA} that is shown connects two parts of the Fermi surface that have parallel tangents, leading to a Kohn anomaly in the scattering rate and the phonon linewidth. A similar process for Nb is illustrated in the lower part of Fig. 1.

In the following calculations, we use an electron-phonon vertex $g_\lambda(\mathbf{k}, \mathbf{k}')$:

$$g_\lambda(\mathbf{k}, \mathbf{k}') = -i \sqrt{\frac{\hbar}{2MN \omega_\lambda(\mathbf{k} - \mathbf{k}')}} \hat{\epsilon}_\lambda(\mathbf{k} - \mathbf{k}') \times \sum_{\mathbf{K}_m, \mathbf{K}_n} (\mathbf{k} + \mathbf{K}_m - \mathbf{k}' - \mathbf{K}_n) a_{\mathbf{K}_m}^\dagger(\mathbf{k}) a_{\mathbf{K}_n}(\mathbf{k}') \times \langle \mathbf{k} + \mathbf{K}_m | U | \mathbf{k}' + \mathbf{K}_n \rangle \quad (1)$$

for a transverse acoustic mode λ that has a frequency $\hbar\omega_\lambda(\mathbf{q})$ and a polarization vector $\hat{\epsilon}_\lambda(\mathbf{q})$. Here M is the ion mass, U is the lattice pseudopotential, and N is the number of lattice sites. As discussed, for transverse phonons one needs an umklapp process to couple the electrons to the direction of the ionic vibration given by $\hat{\epsilon}_{\lambda=T}$. The momentum dependence of the coupling then varies as $g_T(\mathbf{k}, \mathbf{k}') \propto (\mathbf{K} + \mathbf{q}) \cdot \hat{\epsilon}_T \sim \mathbf{K} \cdot \hat{\epsilon}_T$ times a function that is slowly varying for values of \mathbf{k} and \mathbf{k}' that contribute to the Kohn anomaly and which we take as a constant. Then, as we will see, the linewidth of the transverse phonons will exhibit a peak as \mathbf{q} approaches the Kohn anomaly wave vector \mathbf{q}_{KA} .

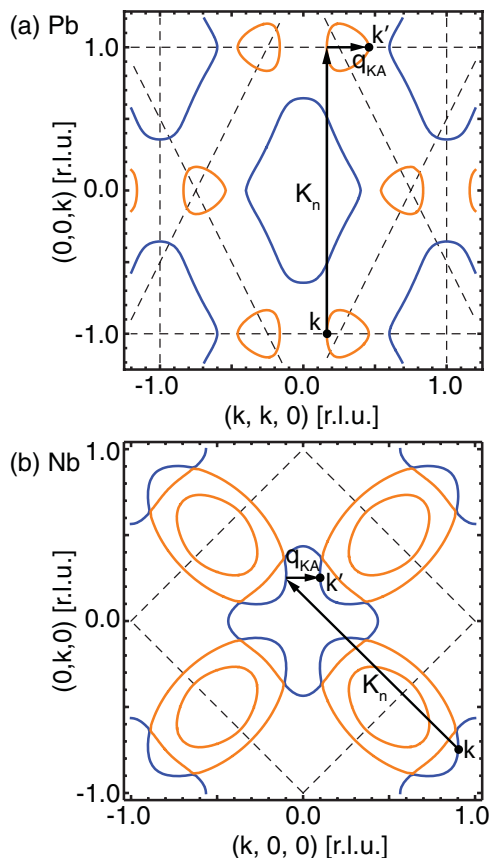


FIG. 1. (Color online) The Fermi surfaces of (a) Pb and (b) Nb. The short black arrows indicate the q_{KA} wave vectors (r.l.u.) $q_{KA} = 0.295$ in Pb and $q_{KA} = 0.196$ in Nb. The long arrow indicates the reciprocal-lattice vector \mathbf{K}_n associated with the umklapp scattering process. The locations of the Bragg planes are indicated by thin dashed lines.

Before proceeding further, we note that the small \mathbf{q} limit is not properly captured by this approximation. On physical grounds one expects $g(\mathbf{k}, \mathbf{k}') \rightarrow 0$ as $\mathbf{q} \rightarrow 0$, as this limit corresponds to a rigid uniform displacement of the lattice and therefore does not couple to the electrons in the periodic potential. As discussed, without umklapp scattering ($\mathbf{K}_n - \mathbf{K}_m = 0$) this limit is satisfied since $g(\mathbf{k}, \mathbf{k}')$ for the transverse modes is identically zero due to momentum conservation. However, once the umklapp scattering processes are included, the coupling constant has a $\mathbf{q} \rightarrow 0$ dependence given by $g(\mathbf{k}, \mathbf{k}') \sim \mathbf{K} \cdot \hat{\epsilon}_T(\mathbf{q}) / \sqrt{\omega(\mathbf{q})}$ times the matrix element appearing in Eq. (1). In this case, a self-consistent determination of the matrix element cancels the $1/\mathbf{q}$ dependence arising from the phonon dispersion such that the proper limit is obtained. However, since our focus is on the phonon lifetime for $\mathbf{q} \sim \mathbf{q}_{KA}$, we proceed with the constant coupling approximation and restrict ourselves to momentum transfers where this approximation is expected to be valid.

To capture the essence of the Kohn-umklapp scattering, we first consider the expression for the transverse acoustic phonon linewidth $\Gamma(\mathbf{q}, T)$ in the normal state for the case in which the Fermi surface spanned by \mathbf{q}_{KA} is approximated by a cylinder

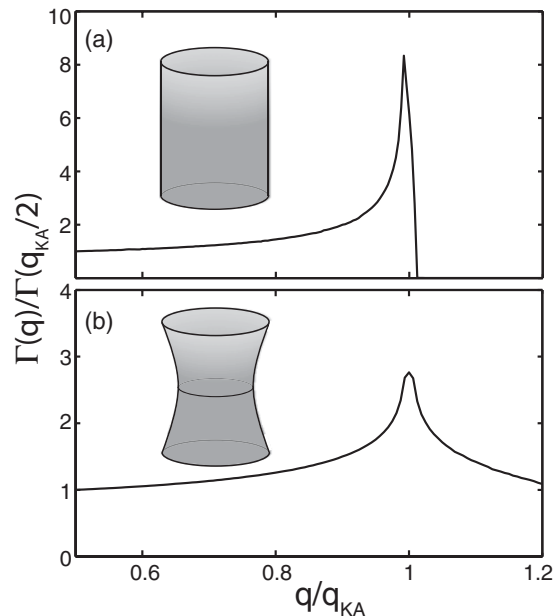


FIG. 2. The normal state $T = 0$ phonon linewidth of the transverse acoustic branch with $c_T/v_F = 0.01$ evaluated for free electrons with (a) a cylindrical Fermi surface and (b) a concave Fermi surface. In both cases, $\Gamma(\mathbf{q})$ has been normalized to its value at $\mathbf{q}_{KA}/2$.

of radius k_F [Fig. 2(a)]. In this case, $\Gamma(\mathbf{q}, T)$ is given by

$$\Gamma(\mathbf{q}, T) = \frac{\pi |g_{\mathbf{k}}|^2}{N} \sum_{\mathbf{k}} [f(\epsilon_{\mathbf{k}}) - f(\epsilon_{\mathbf{k}+\mathbf{q}})] \times \delta(\omega_{\mathbf{q}} - \epsilon_{\mathbf{k}+\mathbf{q}} + \epsilon_{\mathbf{k}}) \quad (2)$$

with f the Fermi factor and $\epsilon_{\mathbf{k}}$ the electronic band dispersion. From here on we choose $\hbar = 1$. For simplicity, we have set $g_{\lambda=T}(\mathbf{k}, \mathbf{k}') = g_{\mathbf{k}}$, the phonon mode energy $\omega_{\mathbf{q}} = c_T |\mathbf{q}|$, with c_T the transverse speed of sound, and we assumed a simple two-dimensional (2D) free-electron dispersion $\epsilon_{\mathbf{k}} = k^2/2m - \mu$. Taking the $T = 0$ limit and making the change of variables $x = k/k_F$, Eq. (2) reduces to

$$\Gamma(\mathbf{q}, T = 0) = \frac{mk_F |g_{\mathbf{k}}|^2}{4\pi q} \int_0^1 x dx \int_0^{2\pi} d\phi [\delta(\alpha_-(\mathbf{q}) - x \cos(\phi)) - \delta(\alpha_+(\mathbf{q}) - x \cos(\phi))], \quad (3)$$

where $\alpha_{\pm}(\mathbf{q}) = \frac{c_T}{v_F} \pm \frac{q}{2k_F}$ and k_F and v_F are the Fermi momentum and velocity, respectively. After a little algebra, we then obtain

$$\Gamma(\mathbf{q}, T = 0) = N_F |g_{\mathbf{k}}|^2 \frac{2k_F}{q} [\sqrt{1 - \alpha_-^2(\mathbf{q})} \Theta(1 - \alpha_-^2(\mathbf{q})) - \sqrt{1 - \alpha_+^2(\mathbf{q})} \Theta(1 - \alpha_+^2(\mathbf{q}))], \quad (4)$$

where N_F is the single-particle density of states per spin at the Fermi level and $\Theta(x)$ is the usual step function.

$\Gamma(\mathbf{q}, T = 0)$ is plotted in Fig. 2(a) for $c_T/v_F = 0.01$. While the overall magnitude of the linewidth is determined by the ratio of c_T/v_F , the momentum dependence comes from simple phase-space considerations. One can see that the phonon linewidth grows rapidly for momentum transfers approaching $2k_F$ in this example and quickly falls to zero for larger momentum transfers as no phase space is available for

scattering. This strong enhancement of the phonon linewidth in the normal state at \mathbf{q} corresponding to the Kohn anomaly will also be present in the superconducting state, with an additional kinematic constraint imposed by the breaking of Cooper pairs.

The kinematic constraint of phonon decay in the superconducting state brings the energy scale 2Δ directly into play. This is shown in Fig. 3, which sketches quasiparticle scattering across the gap edge 2Δ . Due to the dispersion of the phonon, vertical scattering processes having no net wave vector transfers are kinematically forbidden. In order to bridge the gap, the energy of the phonon must be at least 2Δ . In other words, a finite wave-vector transfer must occur where $q = 2\Delta/c_T$. In addition, the dominant Kohn-umklapp process $\mathbf{k}' - \mathbf{k} = \mathbf{K}_n + \mathbf{q}_{KA}$ involves a momentum transfer of \mathbf{q}_{KA} , which in this sketch is $2k_F$. Thus we have two conditions that lead to the conclusion that when $\omega(\mathbf{q})$ of the transverse acoustic phonon branch equals twice the superconducting gap, or in other words when $q = q_{KA} = 2\Delta/c_T$, an enhancement of the phonon decay will occur.

We next consider the transverse acoustic phonon decay rate in the superconducting state for this cylindrical model using conventional BSC theory.⁴ As is well known, the phonon self-energy can be obtained by evaluating the electron-hole bubble.⁸⁻¹¹ In the superconducting state, the phonon self-energy $\Pi(\mathbf{q}, i\omega_m)$ is then given by

$$\Pi(\mathbf{q}, i\omega_m) = \frac{1}{N\beta} \text{Tr} \sum_{n, \mathbf{k}} |g_{\mathbf{k}}|^2 \hat{t}_3 \hat{G}(\mathbf{k}, i\omega_n) \times \hat{G}(\mathbf{k} + \mathbf{q}, i\omega_n + i\omega_m) \hat{t}_3, \quad (5)$$

where $\omega_n = (2n + 1)\pi/\beta$ and $\omega_m = 2m\pi/\beta$ are fermion and boson Matsubara frequencies, Tr denotes the trace, and \hat{G} is the electron propagator,

$$\hat{G}(\mathbf{k}, i\omega_n) = \frac{i\omega_n \hat{t}_0 + \epsilon_{\mathbf{k}} \hat{t}_3 + \Delta_{\mathbf{k}} \hat{t}_1}{(i\omega_n)^2 - E_{\mathbf{k}}^2}. \quad (6)$$

Here \hat{t}_i are the usual Pauli matrices and $E_{\mathbf{k}} = \sqrt{\epsilon_{\mathbf{k}}^2 + \Delta_{\mathbf{k}}^2}$ is the quasiparticle energy. After analytic continuation, the phonon self-energy is given by

$$\begin{aligned} \Pi(\mathbf{q}, \omega_q) = & \frac{1}{2N} \sum_{\mathbf{k}} |g_{\mathbf{k}}|^2 \left\{ A_+(\mathbf{k}, \mathbf{q}) [f(E_{\mathbf{k}}) - f(E_{\mathbf{k}+\mathbf{q}})] \left[\frac{1}{\hbar\omega_q - E_{\mathbf{k}} + E_{\mathbf{k}+\mathbf{q}} + i\delta} - \frac{1}{\hbar\omega_q + E_{\mathbf{k}} - E_{\mathbf{k}+\mathbf{q}} + i\delta} \right] \right. \\ & \left. + A_-(\mathbf{k}, \mathbf{q}) [f(-E_{\mathbf{k}}) - f(E_{\mathbf{k}+\mathbf{q}})] \left[\frac{1}{\hbar\omega_q + E_{\mathbf{k}} + E_{\mathbf{k}+\mathbf{q}} + i\delta} - \frac{1}{\hbar\omega_q - E_{\mathbf{k}} - E_{\mathbf{k}+\mathbf{q}} + i\delta} \right] \right\} \end{aligned} \quad (7)$$

with the coherence factors defined as

$$A_{\pm}(\mathbf{k}, \mathbf{q}) = 1 \pm \frac{\epsilon_{\mathbf{k}} \epsilon_{\mathbf{k}+\mathbf{q}} - \Delta_{\mathbf{k}} \Delta_{\mathbf{k}+\mathbf{q}}}{E_{\mathbf{k}} E_{\mathbf{k}+\mathbf{q}}}. \quad (8)$$

The \mathbf{q} -dependent phonon linewidth $\Gamma(\mathbf{q}, T)$ is then determined from the imaginary part of $\Pi(\mathbf{q}, \omega_q)$.

The first two terms in Eq. (7) describe quasiparticle scattering processes. For these processes, the BCS coherence factor A_+ vanishes at the threshold where $\omega = 2\Delta_0$ and $\epsilon_{\mathbf{k}} = \epsilon_{\mathbf{k}+\mathbf{q}}$. This, along with the depletion of the thermal quasiparticle populations as the gap opens, suppresses their contribution to the phonon linewidth. The fourth term in Eq. (7)

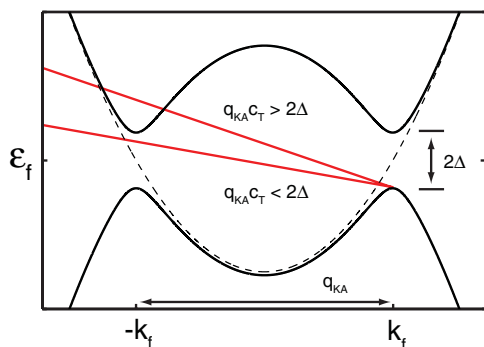


FIG. 3. (Color online) A schematic of the kinematic constraint for the decay of an acoustic phonon in the superconducting state.

corresponds to a process in which a phonon breaks a pair, creating two quasiparticles with wave vectors $\mathbf{k} + \mathbf{q}$ and $-\mathbf{k}$. This requires that the phonon energy $\omega_{\mathbf{q}}$ be greater than or equal to $2\Delta(T)$. In this case, the BCS coherence factor A_- goes to 1 at threshold where $E(\mathbf{k} + \mathbf{q}) = E(\mathbf{k}) = \Delta(T)$ and there is a sudden increase in the linewidth.

Before turning to the results for the linewidth in Pb, we first consider two simplified cases at $T = 0$, shown in Fig. 4. Here we have set the phonon energy $\omega_{\mathbf{q}} = c_T q$ and plotted $\Gamma(\mathbf{q}, T = 0)$ versus q/q_{KA} . The $\Delta = 0$ curve is identical to Fig. 2. As the superconducting gap opens, $\Gamma(\mathbf{q}, T = 0)$ is suppressed for $c_T q < 2\Delta(0)$ due to the loss of phase space for electron-phonon scattering. This produces an onset (or “knee”) in $\Gamma(\mathbf{q}, T = 0)$ at an energy corresponding to the gap edge. Note that in this case one expects a knee rather than a peak because $q\xi \sim v_F/c_T \gg 1$.⁹ (The knee is also somewhat smeared here due to the finite broadening $\delta = c_T/40$ used.)

The height of the onset is controlled by the momentum q for breaking a Cooper pair into two quasiparticles carrying momenta \mathbf{k} and $\mathbf{k} - \mathbf{q}$, respectively.^{7,8} As Δ is made larger, the onset at $c_T q = 2\Delta$ associated with pair-breaking in the superconducting state moves out toward the Kohn anomaly at q_{KA} . For a cylindrical Fermi surface, the Kohn anomaly occurs at $q_{KA} = 2k_F$, and when $2\Delta(0) = c_T q_{KA}$, the pair-breaking onset coincides with the Kohn anomaly peak. If $2\Delta(0)$ exceeds $c_T q_{KA}$, the Kohn anomaly peak is suppressed by kinematics as the energy to break a pair is greater than $c_T q_{KA}$.

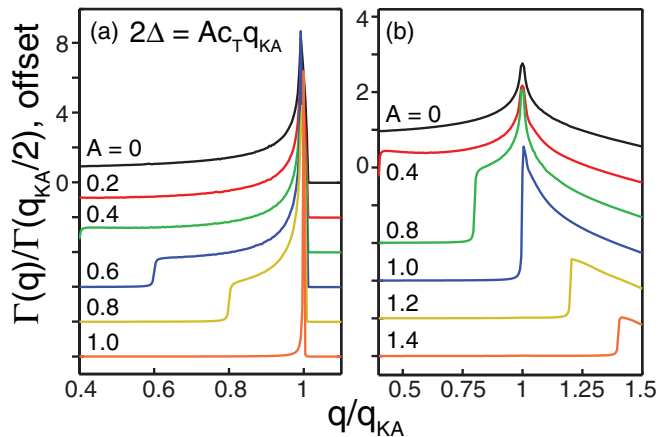


FIG. 4. (Color online) The transverse acoustic phonon linewidth in the superconducting state at $T = 0$ for various values of the superconducting gap $2\Delta = Ac_T q_{KA}$. Each curve has been normalized by the corresponding normal state value at $\mathbf{q}_{KA}/2, T = 0$. (a) $\Gamma(q)$ for a perfectly cylindrical Fermi surface. (b) $\Gamma(q)$ for a cylindrical Fermi surface with a concave warping along the k_z direction (see text).

For a cylindrical Fermi surface with $2\Delta(0) > c_T q_{KA}$, $\Gamma(q)$ is suppressed due to phase-space considerations previously discussed for the normal state. However, if the Fermi surface has some degree of curvature along the k_z direction, such a sharp cutoff will not occur. To illustrate this, in Fig. 4(b) we plot $\Gamma(\mathbf{q}, T = 0)$ for a Fermi surface that has a concave warping along the z direction [see Fig. 2(b)]. The electronic band dispersion has again been modeled by a free electron dispersion but with $m_x = m_y = m$ and $m_z = -5m$.¹² For such a dispersion, q_{KA} corresponds to the spanning condition across the narrowest portion of the Fermi surface ($k_z = 0$). As can be seen in Fig. 4(b), the concave curvature of the Fermi surface provides phase space for scattering with momentum transfers $\mathbf{q} > \mathbf{q}_{KA}$, and the sharp cutoff in $\Gamma(\mathbf{q}, T = 0)$ is no longer present. With the opening of the superconducting gap, $\Gamma(\mathbf{q}, T = 0)$ is suppressed for $c_T q < 2\Delta(0)$, just as in the previous case. For $2\Delta(0) = c_T q_{KA}$, a remnant of the umklapp-Kohn peak remains. As the gap is increased further [$2\Delta(0) > c_T q_{KA}$], the phase space associated with the Kohn peak is gapped out and the peak in $\Gamma(\mathbf{q}, T = 0)$ is thus suppressed.

III. RESULTS FOR LEAD

With the simple examples of the previous sections, we are now ready to turn to the phonon linewidth in Pb. To obtain the electron dispersion, the DFT band structure for Pb was calculated on a regular grid of $100 \times 100 \times 100$ momentum points per quadrant of the first Brillouin zone, and a linear interpolant was used to obtain energies at intermediate momenta. For the phonon dispersion, we again assume a linear phonon dispersion $\omega(\mathbf{q}) = c_T |\mathbf{q}|$, with $c_T = 7.9$ meV/(r.l.u.). The transition temperature $T_c = 7.2$ K sets the temperature scale and we use an intrinsic broadening $\delta = 0.01$ meV throughout. Finally, we note that an explicit evaluation of the matrix element for umklapp scattering $g_{\mathbf{k}, \mathbf{k}'}$ given by Eq. (1) adds a computationally intensive layer to the problem due to

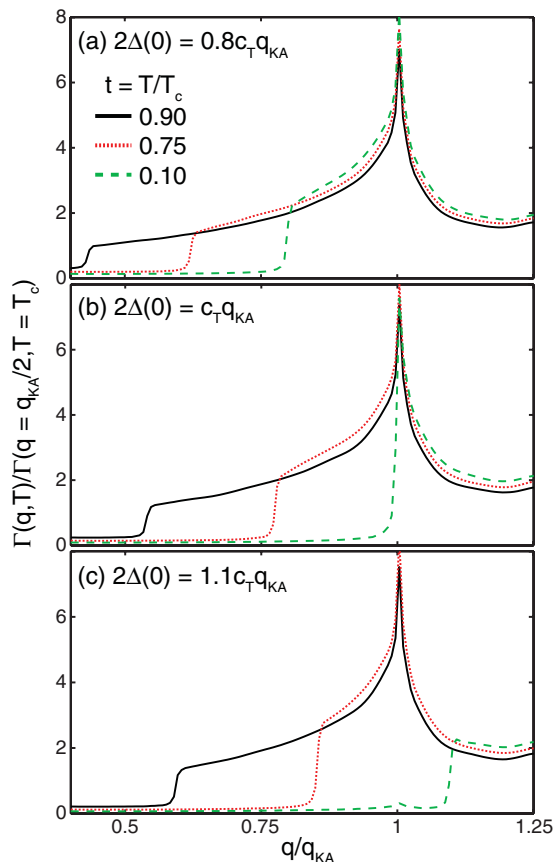


FIG. 5. (Color online) The linewidth of a transverse acoustic phonon in Pb as a function of reduced temperature $t = T/T_c$ for various values of $2\Delta(T = 0)$ as indicated. Each curve has been normalized to the value of the linewidth in the normal state ($T = T_c$) at $\mathbf{q} = \mathbf{q}_{KA}/2$.

the dense momentum grid involved. However, as previously discussed, the momentum dependence of $g(\mathbf{k}, \mathbf{k}')$ is expected to be weak. Therefore, for simplicity, we approximate the matrix element with a constant $g_{\mathbf{k}}$ and restrict the momentum sum to the region near the orange (light) Fermi surfaces shown in Fig. 1(a) while neglecting the contribution from the blue (dark) Fermi surfaces. These cylinder-like orange (light) sections have a large nesting connected by the umklapp wave vector \mathbf{K} and therefore are expected to give the main contribution to the Kohn anomaly due to the large phase space for this scattering process.

The results are shown in Fig. 5 as a function of temperature for gap sizes ranging from $2\Delta(T = 0) = 0.8c_T q_{KA}$ to $1.1c_T q_{KA}$. The qualitative behavior of $\Gamma(\mathbf{q}, T)$ is similar to that found for the simplified models considered in the previous section. Above T_c , the phonon linewidth is finite for all values of $\mathbf{q} = (q, q, 0)$ and has a peak at $q = q_{KA} = 0.285$ (r.l.u.), which is associated with the Kohn anomaly indicated in Fig. 1. As the temperature is lowered across T_c , the gap opens following an assumed BCS temperature dependence. For $c_T q < 2\Delta(T)$, $\Gamma(q, T)$ is suppressed and the expected 2Δ onset (knee) forms. [Here, $\Gamma(\mathbf{q})$ has a finite value for $c_T q < 2\Delta(T)$, which is exponentially suppressed as T is lowered. This is due to the nonzero contributions of the first

TABLE I. The relevant parameters for the elemental superconductors Pb and Nb. The values for Pb have been estimated from Ref. 1. The gap for Nb was obtained from Ref. 14. The transverse speed of sound in Nb was obtained from Ref. 13.

	$2\Delta(0)$ (meV)	c_T (meV/r.l.u.)	q_{KA} (r.l.u.)	$2\Delta(0)/c_T q_{KA}$
Pb	2.70	7.93	0.36	0.95
Nb	3.06	21.3	0.18	0.80

two terms in Eq. (7) and corresponds to the thermal occupation of quasiparticle states across the gap edge.] As T is lowered further, $2\Delta(T)$ grows and the knee in $\Gamma(q, T)$ moves toward the Kohn peak. If $2\Delta(0)$ is smaller than $c_T q_{KA}$, this knee stops short of the peak at the lowest temperatures [Fig. 5(a)], while for $2\Delta(0) = c_T q_{KA}$ it merges with the peak [Fig. 5(b)]. Finally, if $2\Delta(0) > c_T q_{KA}$ [Fig. 5(c)], then for sufficiently low temperatures the Kohn peak is suppressed similar to the results shown in Fig. 4(b).

Thus within a BCS framework, $\Gamma(\mathbf{q}, T)$ depends on the shape of the Fermi surface and \mathbf{q}_{KA} , the velocity of sound for the transverse acoustic branch, and the magnitude of the superconducting gap. The appropriate parameters for Nb and Pb are summarized in Table I. For Pb we estimate $2\Delta(0) = 0.95c_T q_{KA}$, which corresponds closest to Fig. 5(b), while for Nb we estimate $2\Delta(0) = 0.8c_T q_{KA}$, corresponding to Fig. 5(a).

Comparing our results to Figs. 3 and 4 of Ref. 1, we find that agreement with the experimental data for Pb is good while agreement for the case of Nb is less clear. For Pb we find $2\Delta(0) \sim 0.95c_T q_{KA}$ and we therefore expect a knee to form in $\Gamma(\mathbf{q}, T)$ that tracks out to the Kohn peak as the temperature is lowered. This behavior is similar to what is observed experimentally (Fig. 3 of Ref. 1). In the case of Nb, $2\Delta(0) \sim 0.80c_T q_{KA}$, and we therefore expect the knee to approach the Kohn peak but stop short at the lowest temperatures, leaving a pronounced knee in the observed linewidth. Examining Fig. 4(b) of Ref. 1, it is difficult to determine if such a knee is present in the data. Finally, we note that our calculations predict that the Kohn peak should be suppressed when $2\Delta(0) > c_T q_{KA}$. Therefore, one clear way to test the conclusions of this work would be to examine the linewidth of the transverse acoustic branch in a material where $c_T q_{KA} < 2\Delta(0)$.

IV. CONCLUSIONS

We have seen that the momentum and temperature dependence of the transverse acoustic phonon linewidth $\Gamma(\mathbf{q}, T)$ in the superconducting state depends on $\omega_{\mathbf{q}_{KA}}$ and $2\Delta(T)$. While both of these energies depend upon the band structure and phonon dispersion, there is nothing that should lock them together in the traditional theory, particular since the e-ph coupling to this mode in Pb is small.⁴ Thus while it is known that the Kohn anomaly wave vector \mathbf{q}_{KA} shown in Fig. 1 gives rise to a small kink in $\alpha^2 F(\omega)$ associated with the energy $\omega_{\mathbf{q}_{KA}}$ at which the transverse phonon begins to contribute to the pairing interaction, this is a small feature and plays no role in determining the magnitude of $\Delta(0)$.⁴ Therefore, within the BCS framework, the fact that $2\Delta(0)$ is close to the energy of a Kohn anomaly $\omega_{\mathbf{q}_{KA}}$ must be viewed as a coincidence. Furthermore, as noted, the fact that the wavelength of the phonon is small compared to the coherence length leads to a kneelike feature at $2\Delta(0)$ rather than a peak. Therefore, if $\omega_{\mathbf{q}_{KA}} > 2\Delta(0)$, the Kohn anomaly remains as the dominant feature at low temperatures. However, as shown in Figs. 4(b) and 5(a), if $2\Delta(0)$ is slightly less than the Kohn anomaly phonon energy $\omega_{\mathbf{q}_{KA}}$, the $2\Delta(T)$ structure can appear to merge with the Kohn anomaly peak in $\Gamma(\mathbf{q}, T)$ as T goes to zero. Thus we would conclude that it is an interesting coincidence that $2\Delta(0)$ is only slightly smaller than the energies of the Kohn anomalies in both Pb and Nb, but it does not mean that the superconducting gap is determined by the Kohn anomaly itself and does not force $2\Delta(0) = \omega_{\mathbf{q}_{KA}}$.

ACKNOWLEDGMENTS

We would like to acknowledge B. Keimer for useful discussions. This work was supported (A.P.S., B.M., and T.P.D.) by the US Department of Energy, Office of Basic Energy Sciences under Contract No. DE-AC02-76SF00515. D.J.S. acknowledges the Center for Nanophase Materials Science, which is sponsored at Oak Ridge National Laboratory by the Division of Scientific User Facilities, US Department of Energy and thanks the Stanford Institute of Theoretical Physics for their hospitality. S.J. would like to acknowledge financial support from the Natural Sciences and Engineering Research Council of Canada and the Foundation for Fundamental Research on Matter (The Netherlands). S.J., B.M., and T.P.D. would also like to thank the Walther Meissner Institute for their hospitality during the writing of this manuscript.

*Lawrence Livermore National Laboratory, Livermore, California 94550, USA.

¹P. Aynajian, T. Keller, L. Boeri, S. M. Shapiro, K. Habicht, and B. Keimer, *Science* **319**, 1509 (2008).

²W. Kohn, *Phys. Rev. Lett.* **2**, 393 (1957).

³J. Bardeen, L. N. Cooper, and J. R. Schrieffer, *Phys. Rev.* **108**, 1175 (1957).

⁴W. L. McMillan and J. M. Rowell, *Phys. Rev. Lett.* **14**, 108 (1965); *Superconductivity*, edited by R. Parks (Dekker, New York, 1969),

Vol. 1, Chap. 11; D. J. Scalapino, *Superconductivity*, edited by R. Parks (Dekker, New York, 1969), Vol. 1, Chap. 10.

⁵X. Gonze, B. Amadon, P.-M. Anglade, J.-M. Beuken, F. Bottin, P. Boulanger, F. Bruneval, D. Caliste, R. Caracas, M. Côté, T. Deutsch, L. Genovese, Ph. Ghosez, M. Giantomassi, S. Goedecker, D. R. Hamann, P. Hermet, F. Jollet, G. Jomard, S. Leroux, M. Mancini, S. Mazevet, M. J. T. Oliveira, G. Onida, Y. Pouillon, T. Rangel, G.-M. Rignanese, D. Sangalli, R. Shaltaf, M. Torrent, M. J. Verstraete, G. Zerah, and J. W. Zwanziger,

[Comput. Phys. Commun.](#) **180**, 2582 (2009). For both metals, the total energy was converged to 10^{-7} Hartree to obtain a density. The converged calculations used 145 and 220 \mathbf{k} points in the irreducible Brillouin zone, and plane-wave energy cutoffs of 30 and 45 Hartree were used for Pb and Nb, respectively.

⁶J. R. Anderson and V. A. Gold, [Phys. Rev.](#) **139**, A1459 (1965).

⁷D. P. Karim, J. B. Ketterson, and G. W. Crabtree, [J. Low Temp. Phys.](#) **30**, 389 (1978).

⁸T. P. Devereaux and R. Hackl, [Rev. Mod. Phys.](#) **79**, 175 (2007).

⁹M. V. Klein and S. B. Dierker, [Phys. Rev. B](#) **29**, 4976 (1984).

¹⁰F. Marsiglio, R. Akis, and J. P. Carbotte, [Phys. Rev. B](#) **45**, 9865 (1992).

¹¹P. B. Allen, N. Kostur, N. Takesue, and G. Shirane, [Phys. Rev. B](#) **56**, 5552 (1997).

¹²The values of the mass will affect the structure in $\Gamma(q)$ for $q > q_{KA}$ and specifically how quickly it falls off at large \mathbf{q} . It does not change the qualitative features arising from the opening of the gap, which we wish to discuss here.

¹³M. Holt, P. Czoschke, H. Hong, P. Zschack, H. K. Birnbaum, and T.-C. Chiang, [Phys. Rev. B](#) **66**, 064303 (2002).

¹⁴J. P. Carbotte, [Rev. Mod. Phys.](#) **62**, 1027 (1990).